Published in final edited form as:
Biochemistry. 2010 March 23; 49(11): 2317–2325. doi:10.1021/bi901488d.

Kinetics of mismatch formation opposite lesions by the replicative DNA polymerase from bacteriophage RB69

Matthew Hogg[‡], **Jean Rudnicki**[‡], **John Midkiff**[‡], **Linda Reha-Krantz**[§], **Sylvie Doublié**[‡,*], and **Susan S. Wallace**[‡,*]

[‡] Department of Microbiology and Molecular Genetics, 95 Carrigan Drive, University of Vermont, Burlington, VT, 05405, USA

[§] Department of Biological Sciences, CW 405 Biological Sciences Bldg., University of Alberta, Edmonton, Alberta, T6G 2E9, Canada

Abstract

The fidelity of DNA replication is under constant threat from the formation of lesions within the genome. Oxidation of DNA bases leads to the formation of altered DNA bases such as 8-oxo-7,8-dihydroguanine, commonly called 8-oxoG, and 2-hydroxyadenenine, or 2-OHA. In this work we have examined the incorporation kinetics opposite these two oxidatively derived lesions as well as an abasic site analog by the replicative DNA polymerase from bacteriophage RB69. We compared the kinetic parameters for both wild type and the low fidelity L561A variant. While nucleotide incorporation rates (k_{pol}) were generally higher for the variant, the presence of a lesion in the templating position reduced the ability of both the wild type and variant DNA polymerases to form ternary enzyme-DNA-dNTP complexes. Thus, the L561A substitution does not significantly affect the ability of the RB69 DNA polymerase to recognize damaged DNA; instead the mutation increases the probability that nucleotide incorporation will occur. We have also solved the crystal structure of the L561A variant forming an 8-oxoG•dATP mispair and show that the propensity for forming this mispair depends on an enlarged polymerase active site.

Most replicative DNA polymerases copy DNA with high fidelity. These faithful enzymes must select the correct dNTP among the four canonical nucleotides and do so at rates high enough to support replication of the genome within the time frame of a single cell division. The error rates of replicative DNA polymerases range as high as one error for every 10^6 incorporation events (1). While DNA polymerases have the ability to efficiently discriminate between correct and incorrect incoming nucleoside triphosphates, the genomes of all organisms are under constant assault from both endogenous and exogenous sources. The resulting alterations to the genome can have a dramatic effect on the ability of DNA polymerases to maintain accurate DNA replication or to maintain any replication at all (2). Abasic sites are produced at a rate of >10,000 per human cell per day (3). These lesions arise primarily through spontaneous hydrolysis of the *N*-glycosylic bond and as intermediates in the base excision repair pathway (4). Abasic sites (Figure 1) are strong blocks to DNA replication by most replicative DNA polymerases and can only be bypassed at a low rate *in vitro* in the presence of high dNTP concentrations. Under these conditions, all replicative polymerases tested to date exhibit a strong preference for incorporation of dAMP, regardless of the nature of the original templating base. This phenomenon, known as the A-rule, is mutagenic (5,6).

* to whom correspondence should be addressed swallace@uvm.edu or sdoublie@uvm.edu tel: 802-656-2164 fax: 802-656-8749.

Reactive oxygen species pose another significant threat to DNA. In particular, 8-oxo-7,8-dihydroguanine (8-oxoG)[1] is a commonly formed oxidatively derived lesion that has the potential to miscode (Figure 1). Replicative DNA polymerases are reported to bypass templating 8-oxoG, although not as efficiently as G, and many show high rates of dAMP misincorporation instead of incorporating the correct dCMP (7-9). For the 8-oxoG•dCTP pairing, the templating 8-oxoG adopts the usual *anti* conformation and participates in a canonical Watson-Crick base pair (9,10); however 8-oxoG can also adopt the *syn* conformation (11), which allows formation of a Hoogsteen base pair with dATP (12). The resulting mispair presents a minor groove arrangement that is virtually indistinguishable from the normal G•C Watson-Crick base pair such that the DNA polymerase is unable to recognize the mismatch as an error and proceeds with replication (13). The same agents that produce 8-oxoG also produce 2-hydroxyadenine (2-OHA), a lesion that is also capable of miscoding and acting as a pre-mutagenic lesion (14,15) (Figure 1). Although highly sensitive assays have shown little or no production of 2-OHA except under conditions of very high concentrations of Fe^{2+} (16), 2-OHA is stable and readily available, and can be used to probe the determinants of fidelity within the polymerase active site. Moreover, oxidatively derived lesions such as 8-oxoG have been implicated in cancer, aging (17) and neurodegenerative diseases such as Parkinson's (18).

The prevalence of abasic sites and oxidatively derived lesions make them obvious substrates to probe the determinants of fidelity within the active site of replicative DNA polymerases. Crystal structures of replicative DNA polymerase from bacteriophage RB69 have been determined in an *apo* form (19), in complex with DNA in both the polymerizing mode (20) and editing mode (21), and in complex with DNA containing the lesions 8-oxoG (9), thymine glycol (22) or an abasic site (9,23-25). These structures, in combination with biochemical studies (26-28), have shown roles for several key amino acids in forming the tight active site binding pocket. The upper wall of the RB69 DNA polymerase active site comprises two residues, K560 and L561, but only one, L561, is in position to contribute to fidelity by possible steric exclusion of deviations in the templating base. Substitution of the leucine at position 561 with an alanine increases mispair formation *in vitro* and the DNA polymerase variant displays a mutator phenotype *in vivo* (29).

In the work presented here, we have used the RB69 DNA polymerase to examine how replicative DNA polymerases distinguish a blocking lesion, such as an abasic site, from lesions that can be bypassed, *e.g.* 8-oxoG and 2-OHA. We have employed primer extension assays to investigate the effects of these lesions on incorporation by the L561A DNA polymerase. We show that, when compared to the wild type polymerase, the L561A variant exhibits significantly higher rates of catalysis for mispair formation opposite these lesions whereas the binding affinity for the incoming nucleotides is quite low for all mispairs for both the wild type and L561A polymerases. These results are in marked contrast to the results for mispair formation using undamaged bases in which both catalysis rates and binding affinities were altered for various mispairs (29). The crystal structure of the L561A DNA polymerase in complex with a templating 8-oxoG and an incoming dATP suggests that the increased space within the polymerase active site may allow for greater flexibility of the DNA backbone. Our work suggests that when a lesion is present in the template, the enzyme is predisposed to reject the incoming nucleoside triphosphate but when ternary complexes do form, an increased active site volume allows for faster rates of incorporation.

[1]Abbreviations used in this text: 8-oxoG, 8-oxo-7,8-dihydroguanine; 2-OHA, 2-hydroxyadenine; F, tetrahydrofuran; dNTP, deoxyribonucleoside triphosphate; gp43, gene product 43; PEG, polyethylene glycol.

MATERIALS AND METHODS

Materials

All chemicals and reagents were from Sigma (St. Louis, MO) or Fisher (Waltham, MA) and were of the highest purity. Nucleoside triphosphates were purchased from New England Biolabs (Ipswich, MA). The oligonucleotides were synthesized by the Midland Certified Reagent Company (Midland, TX) and were purified on 16% polyacrylamide gels and desalted on Sep-Pak C18 cartridges (Waters Corp., Milford, MA). The sequence of the primer was 5′-GCGGCTGTCATAAG-3′ and the 5′ end of the primer strand was labeled with tetrachlorofluorescein (TET) for subsequent visualization. The template sequence was 5′-GACCAXCTTATGACAGCCGCG-3′ where X denotes a thymine (T), 2-OHA, 8-oxoG or tetrahydrofuran (furan, F), an abasic site analog that is resistant to cleavage (30) and has been used in prior structural studies (9,23-25) (Fig. 1). The sequence used in these experiments is the same as that in previous structural work with an abasic site (24). Primer and template oligonucleotides were annealed in 10 mM Tris pH 7.5, 50 mM NaCl and 1 mM EDTA with a 20% excess of template strand by heating to 70°C and cooling. All duplex oligonucleotides were tested to ensure that at least 90% of the primers were extendable. The plasmid encoding wild type RB69 DNA polymerase gene was provided by Dr. Jim Karam (Tulane University) and that encoding the L561A variant by Dr. William Konigsberg (Yale University).

Methods

Both the wild type and L561A polymerases possess a C-terminal 6-His tag and were purified and stored as previously described (31). All enzymes used in these experiments are the exonuclease deficient D222A, D327A double mutants and wild type refers to the polymerase possessing a leucine at position 561.

The kinetics assays were all performed on an RQF3 rapid quench flow device (KinTek Corp., State College, PA). Syringe A contained 2000 nM gp43 (wild type or L561A) and 500 nM primer/template duplex in 25 mM Tris acetate pH 7.5, 50 mM NaCl, 5 mM β-mercaptoethanol and 0.1 mM EDTA. Syringe B contained 20 mM magnesium acetate and varying concentrations of dNTPs in the same reaction buffer. Upon rapid mixing in the RQF3, the final reactant concentrations were 1000 nM gp43, 250 nM DNA duplex, 10 mM Mg^{2+} and dNTPs ranging from 0.02 mM to 4.5 mM. All reactions were run at 25° C and quenched in 0.5 mM EDTA. Maximal nucleotide incorporation rates were achieved with a ratio of 4 DNA polymerase molecules to 1 DNA substrate. Under such saturating conditions of enzyme excess over DNA substrate, single turnover conditions are ensured and post-chemistry steps and enzyme/DNA dissociation events can be effectively ignored thus allowing estimation of k_{pol} for all reactions (32), These conditions also produced the highest amplitude for the burst rate for nucleotide incorporation reactions with the undamaged template (data not shown). Extended primers were separated from unextended primers on 16% denaturing polyacrylamide gels and the resulting bands were visualized by scanning the gels at 532 nm in a Molecular Imager FX (Bio-Rad, Hercules, CA) to excite the 5′ TET fluorophore. Band intensities were measured with the Quantity-One software package (Bio-Rad) and the amount of product formed was calculated as the ratio of intensities for extended primers over the intensities of both extended and unextended primers. The product formation curves for all slow reactions (rate constants <10 s^{-1}) were best fit to a single exponential equation ($P = A(1-e^{-k*t})$) to yield the observed rate constant k_{obs}. Curves for the fast reactions (rate constants >10 s^{-1}) were best fit to a double exponential equation ($P = A(1-e^{-k_{fast}*t}) + B(1-e^{-k_{slow}*t})$) to yield two rate constants, k_{fast} and k_{slow}. The k_{obs} and k_{fast} values were plotted against dNTP concentration and the resulting curve was fit to a hyperbola ($k_{obs} = (k_{pol}[dNTP]) / (K_{D,APP} + [dNTP])$) to yield the maximal rate constant, k_{pol}, and the apparent dissociation constant for the incoming nucleotide, $K_{D,APP}$. The $K_{D,APP}$ measured here encompasses several steps in the reaction

pathway and is not the ground state nucleotide dissociation constant as determined by other methods (33,34). All curve fits were performed in Prism 5 (GraphPad Software, La Jolla CA).

Ternary complexes of L561A-8-oxoG-dATP were formed by mixing the exonuclease deficient variant (D222A; D327A) (RB69 exo$^-$) of RB69 gp43 (24) (10 mg/ml) with 120 μM primer (5′-GCGGCTGTCATAAG-3′) / template (5′-GCGCCGACAGTATTC(8-oxoG)AC-3′) duplex DNA and 250 μM dideoxyGTP in 6 mM $MnCl_2$, 2 mM dithiothreitol, 6.5 mM HEPES pH 7 and 33 mM NaCl. After 30 minutes at room temperature, the polymerase had chain-terminated all of the primers by incorporating dideoxyGTP (data not shown). dATP was then added to a final concentration of 10 mM and incubated on ice for 30 minutes. Hanging drops were made by mixing 0.5 μl of this reaction mix with 0.5 μl reservoir solution (3% (w/v) PEG 20,000 (Hampton Research, Aliso Viejo CA), 100 mM sodium acetate, 100 mM manganese acetate, 100 mM Tris-HCl pH 7.0, 1% (v/v) glycerol and 5 mM β-mercaptoethanol). Crystals of approximately 100 microns per side grew in about 2 days at 24°C and were quickly dipped into a cryoprotecting solution (4% (w/v) PEG 20,000, 100 mM sodium acetate, 100 mM manganese acetate, 100 mM Tris-HCl pH 7.0, 18 % (v/v) glycerol and 10 mM dATP) prior to flash cooling in liquid nitrogen.

Crystallographic data were collected at beamline 23-Id-B at the Advanced Photon Source (Argonne National Laboratories) and were indexed and scaled using HKL2000 (35). Molecular replacement in Phaser (36) with the A•dTTP ternary complex (20) stripped of all non-protein atoms yielded a starting model that was refined with CNS 1.2 (37) followed by several iterative rounds of model building in Coot (38) and energy minimization in CNS 1.2. Water molecules were picked with CNS 1.2 and final TLS and coordinate refinement was performed with Refmac5.6 (39). The quality of the model was assessed with PROCHECK (40), which shows one residue (threonine 622) in the disallowed region of the Ramachandran plot as seen in previous RB69 DNA polymerase structures (20,24). Coordinates have been deposited with the Protein Data Bank with ID code 3LDS.

RESULTS

Kinetic parameters for incorporation of dNMPs opposite template T and the damaged bases were determined by rapid chemical quench experiments. Rate constants for nucleotide incorporation (k_{pol}) and $K_{D,APP}$ values were determined from the initial burst phases for several dATP concentrations ranging from 2 to 200 μM. For the wild type RB69 DNA polymerase, k_{pol} was ~229 s^{-1} and $K_{D,APP}$ was ~ 21 μM and similar values were observed for the L561A-DNA polymerase with k_{pol} ~252 s^{-1} and $K_{D,APP}$ ~ 13 μM (Table 1). These values are similar to those obtained previously for formation of a dAMP•dTTP basepair (29). Incorporation of dAMP opposite template T by the wild type RB69 DNA polymerase showed biphasic kinetics and product formation curves were best fit to a double exponential equation. The fast phase was the major reaction observed for both the wild type and mutant enzymes (The amplitudes of the rate constant for the fast phase were > 0.8 for all dNTP concentrations) and includes the rates in the first enzyme turnover for dNTP binding, any conformational changes, and phosphodiester bond formation (41). The rate constants for the fast phase were plotted against dNTP concentrations to yield an estimate for k_{pol}. A minor slower phase (amplitude < 0.2) was observed with a rate constant of 15 to 20 s^{-1}. This slower phase is likely due to dissociation and rebinding events associated with enzyme DNA complexes that are not catalytically competent, perhaps enzymes with DNA bound initially in the exonuclease site that need to dissociate and rebind DNA in the polymerase active site. The rate constant of the slow phase observed here is similar to the values obtained for such processes in the homologous polymerase from bacteriophage T4 (42). We also observed a lack of correlation between incoming nucleotide concentrations and the observed rate of the slow phase (data not shown) suggesting that this rate is measuring a process that is dependent upon the partitioning of DNA

between the active sites of the polymerase prior to addition of dNTPs. Thus this slow phase could be measuring intramolecular switching of the primer terminus between the exonuclease and the polymerase active sites (25,43) or enzyme dissociation from the DNA and rebinding. Irrespective of the source of this slower phase, comparisons between wild type and L561A still allow us to make general statements as to whether polymerization rates or binding affinities are altered by the L561A substitution.

The wild type and mutant DNA polymerases also incorporated dTMP opposite template 2-OHA with biphasic kinetics (again, all amplitudes for the fast phase were > 0.8) (Figure 2), but maximal rates required a high concentration of dTTP, especially for the wild type RB69 DNA polymerase (Table 1). While the pre-steady-state k_{pol} parameter decreased only slightly for the L561A DNA polymerase and just 2-fold for the wild type enzyme compared to replication of non-damaged DNA, the $K_{D,APP}$ values increased ~50-fold (*.68/.013)* and ~80-fold (*1.67/.021*) for the mutant and wild type enzymes respectively. Thus, formation of productive ternary complexes required high dTTP concentrations. Once ternary complexes are formed, however, nucleotide incorporation ensues at rates similar to formation of standard Watson-Crick base pairs.

In contrast, the apparent rate constants for incorporation of any other dNMP opposite template 2-OHA were considerably lower (more than 1000-fold lower for the L561A DNA polymerase and more than 5,000-fold lower for the wild type RB69 DNA polymerase) and $K_{D,APP,}$ values were all above the physiological level. For the less favorable misincorporation reactions, rate constants were 10- to >20-fold lower for the wild type enzyme (Table 1) as was observed previously for formation of mismatches with non-damaged DNA (29). The low k_{pol} values suggest that the population of catalytically competent ternary complexes is small, likely a result of an increased rate of reverse conformation change (closed to open) as defined by k_{-2} in the kinetic scheme of Tsai and Johnson (33).

Since correct replication of 2-OHA is highly favored over incorrect replication by both the wild type and mutant DNA polymerases, this lesion is not predicted to be highly mutagenic in RB69. Replication of 8-oxoG, however, is known to be mutagenic in all organisms. Both the wild type and mutant DNA polymerases catalyzed correct translesion replication, incorporation of dCMP opposite template 8-oxoG, in a biphasic manner as described. The k_{pol} values (as calculated from plots of the rate constants for the fast phase against dCTP concentration) were slightly lower than for the undamaged incorporation of dTTP opposite A but the $K_{D,APP}$ values were significantly higher resulting in an almost 50-fold reduction in the efficiency of incorporating dCTP opposite 8-oxoG (Table 2). Incorporation of dAMP opposite 8-oxoG was the most favored incorrect nucleotide incorporation reaction. Biphasic kinetics were observed for the L561A DNA polymerase, k_{pol} ~33 s^{-1} (again, where the higher rate constant is the major phase), but incorporation of dAMP by the wild type RB69 DNA polymerase occurred with a single rate constant of ~6 s^{-1} (Table 1). The wild type RB69 DNA polymerase favors the correct incorporation of dCMP opposite template 8-oxoG almost 40-fold over incorporation of dAMP while the variant discriminates less, about 10-fold (Table 2).

Replication of abasic sites is not an efficient reaction for either the wild type or mutant DNA polymerases (Table 2, Figure 2). Despite this deficiency, the L561A DNA polymerase shows a higher increase in k_{pol} for incorporation opposite tetrahydrofuran when compared to wild type, especially for incorporating pyrimidines opposite the lesion (Table 1). Like the reactions with 2-OHA and 8-oxoG, the $K_{D,APP}$ values for incorporation opposite the furan were unaffected by the L561A substitution. It should be noted that the abasic site analog used in this study may differ in its conformational flexibility (44) and *in vivo* (45) effects when compared to a naturally occurring 2′-deoxyribose abasic site.

Crystallization trials of ternary complexes of L561A gp43 with duplex DNA containing an oxidatively derived lesion or furan in the templating position and an incoming dNTP were performed to visualize the effect of the L561A substitution on the active site of the polymerase. The only complexes that crystallized opposite 2-OHA were with dTTP as the incoming nucleotide. Likewise with 8-oxoG, the easiest ternary complexes to grow in terms of the number, size, diffraction quality and tolerance for varying growth conditions were with dCTP as the incoming dNTP. The only mismatch that was successfully crystallized was the 8-oxoG•dATP complex reported here. Interestingly, attempts to grow these crystals in the presence of magnesium yielded poorly diffracting crystals whereas addition of manganese produced usable crystals. The kinetics experiments were all performed with magnesium, but it has been shown previously for the homologous polymerase from bacteriophage T4 that manganese dramatically increases k_{pol} values and decreases apparent $K_{D,APP}$ values for forming mismatches and for incorporation opposite abasic sites (46) and a similar effect may be occurring with 8-oxoG.

Crystals of the ternary complex of the L561A DNA polymerase in complex with a templating 8-oxoG and incoming dATP diffracted X-rays to 3.0 Å. The space group is $P2_12_12_1$ and there is one ternary complex per asymmetric unit. Data collection and refinement statistics are shown in Table 3. The DNA primer was chain terminated by incorporation of dideoxyGMP prior to addition of a large excess of dATP and radiolabeling of the reaction mixtures showed no detectable un-extended primer after 30 minutes at room temperature (data not shown).

The overall architecture of the complex is like that observed previously for other RB69 gp43 ternary complexes (9,20,23). The fingers domain is closed, bringing the conserved residues R482, K486 and K560 into contact with the triphosphate tail of the incoming nucleotide and pinning it against the conserved catalytic aspartates D411, and D621 (Fig. 3). Two manganese ions have been placed into the electron density between the catalytic aspartates and the triphosphate tail of the incoming dATP based on the presence of two strong peaks in an anomalous difference Fourier map (Fig. 3). A third manganese is found in the exonuclease active site. Difference maps calculated with the 8-oxoG•dATP residues omitted show clear density for the 8-oxoG residue in a *syn* conformation. The guanine base has rotated around its N-glycosylic bond to place the oxygen atom at position 8 in the minor groove of the DNA and to present its Hoogsteen face to the incoming dATP. The oxygen at position 6 of 8-oxoG is now placed directly opposite the alanine substitution at position 561 (Fig. 3).

DISCUSSION

Replicative DNA polymerases are accurate enzymes capable of efficiently inserting the correct nucleotide opposite the templating base. Oxidation of templating bases, however, can alter the shape, size, and hydrogen bonding capability of the base. Removal of the base altogether to form an abasic site has a dramatic effect on the steric arrangement of the polymerase active site by creating an unfilled void. These DNA lesions can lead to replication fork arrest or, if bypassed incorrectly, contribute to the mutation load of an organism (47).

In this work we have attempted to identify DNA polymerase interactions that prevent replication of damaged DNA by highly accurate replicative DNA polymerases. Three types of lesions were studied *in vitro*: 2-OHA, 8-oxoG, and tetrahydrofuran (Figure 1). Since the wild type RB69 DNA polymerase may display high discrimination against these DNA lesions, we also employed the low fidelity L561A DNA polymerase. The L561A DNA polymerase has an increased ability to allow formation of several incorrect base pairs compared to the wild type RB69 DNA polymerase, including incorporation of dAMP opposite template A and incorporation of dGMP opposite template G with $K_{D,APP}$ values less than 200 μM (29), which is the estimated concentration of dNTPs at phage replication forks (48). The rate constants for

these reactions were generally higher for the DNA polymerase variant, but still ~3 orders of magnitude lower than for incorporation of correct nucleotides. Nevertheless, a weak mutator phenotype is observed for the L561A DNA polymerase *in vivo* that appears to underestimate the magnitude of mismatch formation since synthetic lethality was observed for an exonuclease-deficient L561A DNA polymerase, which was attributed to error catastrophe (29). In other words, most of the mismatches formed by the L561A DNA polymerase may be corrected by exonucleolytic proofreading. Given the potential for mismatch formation by the L561A-DNA polymerase, this variant may also replicate damaged DNA that normally blocks replication by the wild type RB69 DNA polymerase.

In previous work with the L561A variant (29), all mismatches with undamaged templates formed by wild type DNA polymerase exhibited a higher $K_{D,APP}$ than for normal incorporations by at least an order of magnitude. Furthermore the $K_{D,APP}$ for each mismatch, although higher than for normal base pairs, was lower for the L561A variant than for wild type (29). In contrast, when lesions are present the $K_{D,APP}$ values for mismatches are relatively unchanged between wild type and L561A DNA polymerases (Table 1). The only noticeable difference between the L561A variant and wild type is a 2-3 fold reduction in $K_{D,APP}$ values for the canonical 8-oxoG•dCTP and 2-OHA•dTTP pairs and F•dAMP by L561A. This pattern is opposite to that observed for the non-lesion mismatches where the $K_{D,APP}$ values for mismatches were reduced by the L561A variant but little effect was observed for Watson-Crick base pairs (29).

We have observed that the k_{pol} values for incorporating the canonical base opposite a lesion are similar to wild type incorporation rates (202 s^{-1} for incorporating a dTMP opposite 2-OHA by the L561A mutant) to at most three-fold reduced (75 s^{-1} for incorporating a C opposite 8-oxoG by the L561A mutant) while the $K_{D,APP}$ values are at least an order of magnitude greater for these “normal” incorporations (Table 1). Thus, while these polymerases are able to incorporate correct nucleotides opposite oxidatively derived lesions at near wild type rates, their apparent affinity for the incoming nucleotide is significantly reduced. Taken together with the observation that the L561A substitution does not increase nucleotide binding affinity for mismatches opposite lesions but does for mismatches opposite undamaged templates (29), our results suggest that the presence of a lesion in the templating position alters the ground state of the enzyme such that the enzyme/DNA complex is less amenable to binding the incoming nucleotide. While lesions such as 8-oxoG have been shown to be non-distorting within the confines of duplex DNA (49), Structural studies with the T7 DNA polymerase that show the templating 8-oxoG residue to be disordered in binary enzyme/DNA complexes while similar complexes with a templating G are well ordered (13) support our hypothesis.

As noted in the Results, we have been unsuccessful in growing crystals for any mismatch other than 8-oxoG (syn)•dATP, even in the presence of manganese. The only other crystals of a ternary complex with a mismatch in the active site of RB69 DNA polymerase have been grown with 5-nitroindol-triphosphate (5NITP) opposite the lesion (23). 5NITP has been shown to be incorporated opposite abasic sites with kinetic parameters similar to those for incorporation of T opposite A (50). Taken together these results support the hypothesis that attempts at forming mismatches will not result in large populations of stable complexes and are thus not likely to crystallize as closed, ternary complexes (51).

Alignment of the ternary complex with dCTP opposite a templating 8-oxoG (*anti*) (9) onto the α-carbons of the palm domain of the current structure of dATP opposite a templating 8-oxoG (*syn*) is shown in Figure 4. When leucine 561 is modeled into the 8-oxoG (*syn*)•dATP complex it becomes apparent that the presence of the leucine residue may present a steric hindrance to the formation of a 8-oxoG (*syn*)•dATP base pair. Preventing this unfavorable interaction may not be as simple as shifting the position of the leucine residue during the switch from the open

to closed conformations as this residue is held into position through van der Waals contacts with F280, F282 and the aliphatic portion of K279. Thus the truncation of leucine to alanine is necessary for an increased efficiency in incorporating nucleotides opposite templating lesions.

As shown in Figure 5A, leucine 561 fills in a cavity within the polymerase active site lined by residues K279, F280, F282, P361 and S565. When this leucine is substituted with alanine as shown in Figure 5B, the cavity becomes more open and could allow greater freedom of movement of the templating base. Figure 5C shows a model in which S565 has been mutated to glycine as previously described (52) and this cavity is even further enlarged. In these experiments the addition of the G565S mutation to L561A (in addition to Y567A) showed an even greater propensity for the polymerase to tolerate mismatches. It is clear that large conformational changes must occur in templating bases as they switch between *syn* and *anti* conformations; in addition the flexibility of abasic sites has been shown to modulate their ability to pair with different incoming dNTPs (44). We have observed that the L561A substitution has a dramatic effect only in comparison with wild type in forming mismatches opposite lesions. When incorporating a dCTP opposite 8-oxoG or dTTP opposite 2-OHA, major conformational changes are not likely to be required in the templating base and no strong effect is observed by substituting alanine at position 561. Only when mismatches are formed, and rearrangement of the templating base with respect to the incoming nucleotide is likely to be required, do we observe an increase in polymerization rate with the L561A DNA polymerase compared to wild type. With an abasic site in the templating position, the loss of leucine 561 and the opening of the cavity shown in Figure 5 may also allow for greater flexibility of the DNA backbone and allow for rare, but catalytically competent, conformations to develop within the polymerase active site.

Kuchta and co-workers have shown that, for B-Family polymerases such as RB69 gp43, the spatial arrangement of certain amide residues are a major determining factor in fidelity (53). It is likely, therefore, that the L561A mutation allows a greater freedom of movement within the active site such that, upon closing of the fingers, there is a greater possibility, although still a rare event, that the required atoms will be properly positioned to allow chemistry. These rare arrangements of nucleotides are even more pronounced when incorporating opposite abasic sites as these lesions exhibit the largest increase in k_{pol} when comparing L561A to wild type. An increase in volume of the polymerase active site (as in the L561A variant) has been postulated to be a determining factor in the ability of many translesion polymerases to bypass a variety of otherwise blocking or mutagenic lesions (54).

Such an effect on allowing template flexibility does not necessarily have to occur after closing of the fingers domain but may allow for energetically favorable conformations to develop while the fingers domain is in the process of closing. In recent experiments (52) in which the nucleotide binding pocket has been enlarged further than with just the L561A substitution, the authors note that an enlargement of the active site does not necessarily correlate with incorporation efficiency. While unfavorable interactions between leucine 561 and 8-oxoG (*syn*) (Figure 4B) may hamper the ability of the wild type polymerase to form ternary complexes between 8-oxoG and dATP, such interactions are not likely to be involved in incorporations opposite abasic sites where the largest difference in k_{pol} is seen between wild type and the L561A variant (Table 1). Thus the effect of enlarging the polymerase active site may not be observed upon successful closure of the fingers domain, especially if the incoming dNTP helps stabilize the position of the templating base once the closed conformation is formed, but this enlargement may alter the transition from an open to closed conformation. Accordingly, we may not be directly observing an effect of the alanine substitution *per se* in allowing alternate conformations of the template to exist. Instead, increasing the volume of the polymerase active site may simply provide an environment for greater DNA flexibility and the differences in

catalytic rates are actually a measurement of how readily a particular lesion can adopt an alternate conformation to allow for aberrant base pairing schemes such as Hoogsteen or wobble base pairs. Thus lesions such as 8-oxoG may be more amenable to alternate forms as indicated by overall higher k_{pol} rates than 2-OHA, which is perhaps less able in general to assume alternate conformations necessary to form mismatches but can still adopt these conformations more readily with the increase in active site volume provided by the L561A substitution. Such an effect of conformational heterogeneity in forming mismatches opposite 8-oxoG has been observed recently in crystal structures with Dpo4, a translesion DNA polymerase with an enlarged active site compared to high-fidelity replicative DNA polymerases (55).

In summary, we have shown that when the polymerase active site of RB69 DNA polymerase is enlarged by substituting alanine for the leucine at position 561, the polymerase is more efficient at misincorporating nucleotides opposite the oxidation products 8-oxoG and 2-OHA as well as abasic sites. The increase in efficiency derives primarily from an increase in the incorporation rate while the apparent binding affinity for the incoming nucleoside triphosphate remains low for both wild type and the L561A variant. This is in contrast to previous experiments showing that the L561A substitution can increase polymerization rates as well as increase the apparent nucleotide binding affinity for mismatches with undamaged templates (29). We interpret this to suggest a predisposition of the polymerase to reject the lesion containing templates. The crystal structure of the L561A variant in a ternary complex with DNA containing an 8-oxoG as the templating base and an incoming dATP suggests that the L561A substitution may allow for greater conformational flexibility of the template that could account for the increase in polymerization rates when forming mismatches opposite lesions.

Acknowledgments

Polymerase expression and purification were carried out by the ECC Core facility by Wendy Cooper at the University of Vermont. We thank Karl Zahn for assistance in structure refinement, and Dr. Pierre Aller and Karl Zahn for collecting the diffraction data set at the APS synchrotron.

This research was supported by PHS grant CA-52040 awarded by the National Cancer Institute and by a Canadian Institutes of Health Research grant to LR-K. LR-K is a scientist of the Alberta Heritage Foundation for Medical Research. GM/CA CAT has been funded in whole or in part with Federal funds from the National Cancer Institute (Y1-CO-1020) and the National Institute of General Medical Science (Y1-GM-1104). Use of the Advanced Photon Source was supported by the U.S. Department of Energy, Basic Energy Sciences, Office of Science, under contract No. DE-AC02-06CH11357.

REFERENCES

1. McCulloch SD, Kunkel TA. The fidelity of DNA synthesis by eukaryotic replicative and translesion synthesis polymerases. Cell Res 2008;18:148–161. [PubMed: 18166979]
2. Friedberg, EC.; Walker, GC.; Siede, W. DNA repair and mutagenesis. Washington, D.C.; ASM Press: 1995.
3. Lindahl T, Barnes DE. Repair of endogenous DNA damage. Cold Spring Harb Symp Quant Biol 2000;65:127–133. [PubMed: 12760027]
4. Wallace, SS. Oxidative Damage to DNA and its Repair. In: Scandalios, J., editor. Oxidative Stress and the Molecular Biology of Antioxidant Defenses. Cold Spring Harbor Laboratory Press; Cold Spring Harbor, NY: 1997. p. 49-90.
5. Schaaper RM, Kunkel TA, Loeb LA. Infidelity of DNA synthesis associated with bypass of apurinic sites. Proc Natl Acad Sci U S A 1983;80:487–491. [PubMed: 6300848]
6. Loeb LA, Preston BD. Mutagenesis by apurinic/apyrimidinic sites. Annu Rev Genet 1986;20:201–230. [PubMed: 3545059]
7. Shibutani S, Takeshita M, Grollman AP. Insertion of specific bases during DNA synthesis past the oxidation-damaged base 8-oxodG. Nature 1991;349:431–434. [PubMed: 1992344]

8. Cheng KC, Cahill DS, Kasai H, Nishimura S, Loeb LA. 8-Hydroxyguanine, an abundant form of oxidative DNA damage, causes G----T and A----C substitutions. J Biol Chem 1992;267:166–172. [PubMed: 1730583]
9. Freisinger E, Grollman AP, Miller H, Kisker C. Lesion (in)tolerance reveals insights into DNA replication fidelity. EMBO J 2004;23:1494–1505. [PubMed: 15057282]
10. Krahn JM, Beard WA, Miller H, Grollman AP, Wilson SH. Structure of DNA polymerase beta with the mutagenic DNA lesion 8-oxodeoxyguanine reveals structural insights into its coding potential. Structure 2003;11:121–127. [PubMed: 12517346]
11. Uesugi S, Ikehara M. Carbon-13 magnetic resonance spectra of 8-substituted purine nucleosides: characteristic shifts for the syn conformation. J Am Chem Soc 1977;99:3250–3253. [PubMed: 853179]
12. Brieba LG, Kokoska RJ, Bebenek K, Kunkel TA, Ellenberger T. A lysine residue in the fingers subdomain of T7 DNA polymerase modulates the miscoding potential of 8-oxo-7,8-dihydroguanosine. Structure 2005;13:1653–1659. [PubMed: 16271888]
13. Brieba LG, Eichman BF, Kokoska RJ, Doublié S, Kunkel TA, Ellenberger T. Structural basis for the dual coding potential of 8-oxoguanosine by a high-fidelity DNA polymerase. EMBO J 2004;23:3452–3461. [PubMed: 15297882]
14. Kamiya H, Kasai H. Mutations induced by 2-hydroxyadenine on a shuttle vector during leading and lagging strand syntheses in mammalian cells. Biochemistry 1997;36:11125–11130. [PubMed: 9287155]
15. Kamiya H, Ueda T, Ohgi T, Matsukage A, Kasai H. Misincorporation of dAMP opposite 2-hydroxyadenine, an oxidative form of adenine. Nucleic Acids Res 1995;23:761–766. [PubMed: 7708490]
16. Frelon S, Douki T, Cadet J. Radical oxidation of the adenine moiety of nucleoside and DNA: 2-hydroxy-2′-deoxyadenosine is a minor decomposition product. Free Radic Res 2002;36:499–508. [PubMed: 12150538]
17. Ames BN, Gold LS. Endogenous mutagens and the causes of aging and cancer. Mutat Res 1991;250:3–16. [PubMed: 1944345]
18. Nakabeppu Y, Tsuchimoto D, Yamaguchi H, Sakumi K. Oxidative damage in nucleic acids and Parkinson's disease. J Neurosci Res 2007;85:919–934. [PubMed: 17279544]
19. Wang J, Sattar AK, Wang CC, Karam JD, Konigsberg WH, Steitz TA. Crystal structure of a pol alpha family replication DNA polymerase from bacteriophage RB69. Cell 1997;89:1087–1099. [PubMed: 9215631]
20. Franklin MC, Wang J, Steitz TA. Structure of the replicating complex of a pol alpha family DNA polymerase. Cell 2001;105:657–667. [PubMed: 11389835]
21. Shamoo Y, Steitz TA. Building a replisome from interacting pieces: sliding clamp complexed to a peptide from DNA polymerase and a polymerase editing complex. Cell 1999;99:155–166. [PubMed: 10535734]
22. Aller P, Rould MA, Hogg M, Wallace SS, Doublié S. A structural rationale for stalling of a replicative DNA polymerase at the most common oxidative thymine lesion, thymine glycol. Proc Natl Acad Sci U S A 2007;104:814–818. [PubMed: 17210917]
23. Zahn KE, Belrhali H, Wallace SS, Doublié S. Caught bending the A-rule: crystal structures of translesion DNA synthesis with a non-natural nucleotide. Biochemistry 2007;46:10551–10561. [PubMed: 17718515]
24. Hogg M, Wallace SS, Doublié S. Crystallographic snapshots of a replicative DNA polymerase encountering an abasic site. EMBO J 2004;23:1483–1493. [PubMed: 15057283]
25. Hogg M, Aller P, Konigsberg W, Wallace SS, Doublié S. Structural and biochemical investigation of the role in proofreading of a beta hairpin loop found in the exonuclease domain of a replicative DNA polymerase of the B family. J Biol Chem 2007;282:1432–1444. [PubMed: 17098747]
26. Yang G, Franklin M, Li J, Lin TC, Konigsberg W. A conserved Tyr residue is required for sugar selectivity in a Pol alpha DNA polymerase. Biochemistry 2002;41:10256–10261. [PubMed: 12162740]

27. Yang G, Franklin M, Li J, Lin TC, Konigsberg W. Correlation of the kinetics of finger domain mutants in RB69 DNA polymerase with its structure. Biochemistry 2002;41:2526–2534. [PubMed: 11851399]
28. Zakharova E, Wang J, Konigsberg W. The activity of selected RB69 DNA polymerase mutants can be restored by manganese ions: the existence of alternative metal ion ligands used during the polymerization cycle. Biochemistry 2004;43:6587–6595. [PubMed: 15157091]
29. Zhang H, Rhee C, Bebenek A, Drake JW, Wang J, Konigsberg W. The L561A substitution in the nascent base-pair binding pocket of RB69 DNA polymerase reduces base discrimination. Biochemistry 2006;45:2211–2220. [PubMed: 16475809]
30. Takeshita M, Chang CN, Johnson F, Will S, Grollman AP. Oligodeoxynucleotides containing synthetic abasic sites. Model substrates for DNA polymerases and apurinic/apyrimidinic endonucleases. J Biol Chem 1987;262:10171–10179. [PubMed: 2440861]
31. Hogg M, Cooper W, Reha-Krantz L, Wallace SS. Kinetics of error generation in homologous B-family DNA polymerases. Nucleic Acids Res 2006;34:2528–2535. [PubMed: 16687658]
32. Joyce CM. Techniques used to study the DNA polymerase reaction pathway. Biochim Biophys Acta-Proteins and Proteomics. 2009
33. Tsai YC, Johnson KA. A new paradigm for DNA polymerase specificity. Biochemistry 2006;45:9675–9687. [PubMed: 16893169]
34. Zhang H, Cao W, Zakharova E, Konigsberg W, De La Cruz EM. Fluorescence of 2-aminopurine reveals rapid conformational changes in the RB69 DNA polymerase-primer/template complexes upon binding and incorporation of matched deoxynucleoside triphosphates. Nucleic Acids Res 2007;35:6052–6062. [PubMed: 17766250]
35. Otwinowski Z, Minor W. Processing of X-ray diffraction data collected in oscillation mode. Methods in Enzymology 1997;276:307–326.
36. McCoy AJ, Grosse-Kunstleve RW, Adams PD, Winn MD, Storoni LC, Read RJ. Phaser crystallographic software. J Appl Crystallogr 2007;40:658–674. [PubMed: 19461840]
37. Brunger AT. Version 1.2 of the Crystallography and NMR system. Nat Protoc 2007;2:2728–2733. [PubMed: 18007608]
38. Emsley P, Lohkamp B, Scott W, Cowtan K. Features and development of COOT. Acta Crystallogr D Biol Crystallogr 2010;66
39. Winn MD, Murshudov GN, Papiz MZ. Macromolecular TLS refinement in REFMAC at moderate resolutions. Methods Enzymol 2003;374:300–321. [PubMed: 14696379]
40. Laskowski RA, Macarthur MW, Moss DS, Thornton JM. PROCHECK: a program to check the stereochemical quality of protein structures. Journal of Applied Crystallography 1993;26:283–291.
41. Hariharan C, Bloom LB, Helquist SA, Kool ET, Reha-Krantz LJ. Dynamics of nucleotide incorporation: snapshots revealed by 2-aminopurine fluorescence studies. Biochemistry 2006;45:2836–2844. [PubMed: 16503638]
42. Wu P, Nossal N, Benkovic SJ. Kinetic characterization of a bacteriophage T4 antimutator DNA polymerase. Biochemistry 1998;37:14748–14755. [PubMed: 9778349]
43. Donlin MJ, Patel SS, Johnson KA. Kinetic partitioning between the exonuclease and polymerase sites in DNA error correction. Biochemistry 1991;30:538–546. [PubMed: 1988042]
44. Chen J, Dupradeau FY, Case DA, Turner CJ, Stubbe J. DNA oligonucleotides with A, T, G or C opposite an abasic site: structure and dynamics. Nucleic Acids Res 2008;36:253–262. [PubMed: 18025040]
45. Kroeger KM, Goodman MF, Greenberg MM. A comprehensive comparison of DNA replication past 2-deoxyribose and its tetrahydrofuran analog in Escherichia coli. Nucleic Acids Res 2004;32:5480–5485. [PubMed: 15477395]
46. Hays H, Berdis AJ. Manganese substantially alters the dynamics of translesion DNA synthesis. Biochemistry 2002;41:4771–4778. [PubMed: 11939771]
47. Yu SL, Lee SK, Johnson RE, Prakash L, Prakash S. The stalling of transcription at abasic sites is highly mutagenic. Mol Cell Biol 2003;23:382–388. [PubMed: 12482989]
48. Sinha NK, Morris CF, Alberts BM. Efficient in vitro replication of double-stranded DNA templates by a purified T4 bacteriophage replication system. J Biol Chem 1980;255:4290–4293. [PubMed: 6989836]

49. Oda Y, Uesugi S, Ikehara M, Nishimura S, Kawase Y, Ishikawa H, Inoue H, Ohtsuka E. NMR studies of a DNA containing 8-hydroxydeoxyguanosine. Nucleic Acids Res 1991;19:1407–1412. [PubMed: 2027747]
50. Reineks EZ, Berdis AJ. Evaluating the contribution of base stacking during translesion DNA replication. Biochemistry 2004;43:393–404. [PubMed: 14717593]
51. Joyce CM, Benkovic SJ. DNA polymerase fidelity: kinetics, structure, and checkpoints. Biochemistry 2004;43:14317–14324. [PubMed: 15533035]
52. Zhang H, Beckman J, Wang J, Konigsberg W. RB69 DNA polymerase mutants with expanded nascent base-pair-binding pockets are highly efficient but have reduced base selectivity. Biochemistry 2009;48:6940–6950. [PubMed: 19522539]
53. Patro JN, Urban M, Kuchta RD. Role of the 2-amino group of purines during dNTP polymerization by human DNA polymerase alpha. Biochemistry 2009;48:180–189. [PubMed: 19072331]
54. Yang W, Woodgate R. What a difference a decade makes: insights into translesion DNA synthesis. Proc Natl Acad Sci U S A 2007;104:15591–15598. [PubMed: 17898175]
55. Rechkoblit O, Malinina L, Cheng Y, Geacintov NE, Broyde S, Patel DJ. Impact of conformational heterogeneity of oxoG lesions and their pairing partners on bypass fidelity by Y family polymerases. Structure 2009;17:725–736. [PubMed: 19446528]

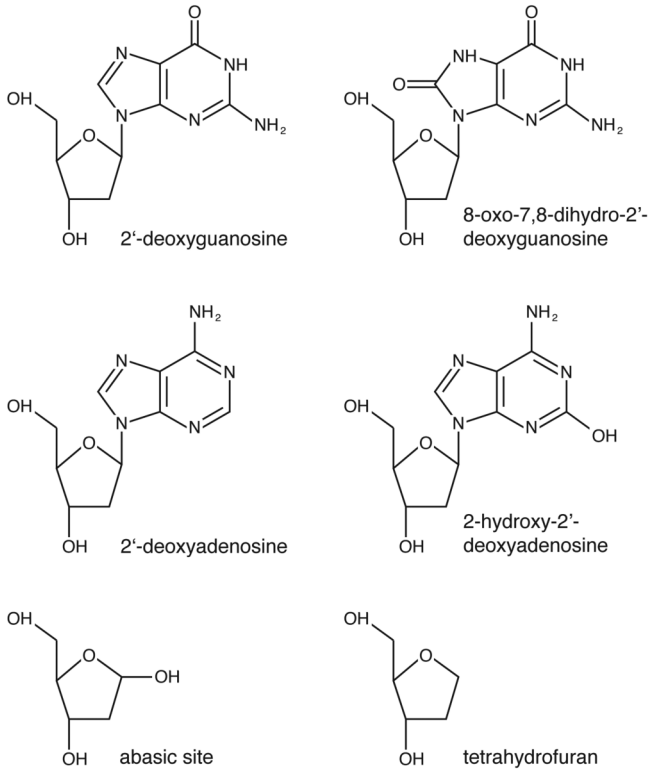

Figure 1.

The lesions studied in this work. *Top:* The oxidation of 2′-deoxyguanosine leads to 8-oxo-7,8-dihydro-2′-deoxyguanosine. *Middle:* The oxidation of 2′-deoxyadenosine generates 2-hydroxy-2′-deoxyadenosine. *Bottom:* A naturally occurring abasic site (hemiacetal form) (left) and a non-hydrolyzable form, tetrahydrofuran (F) (right).

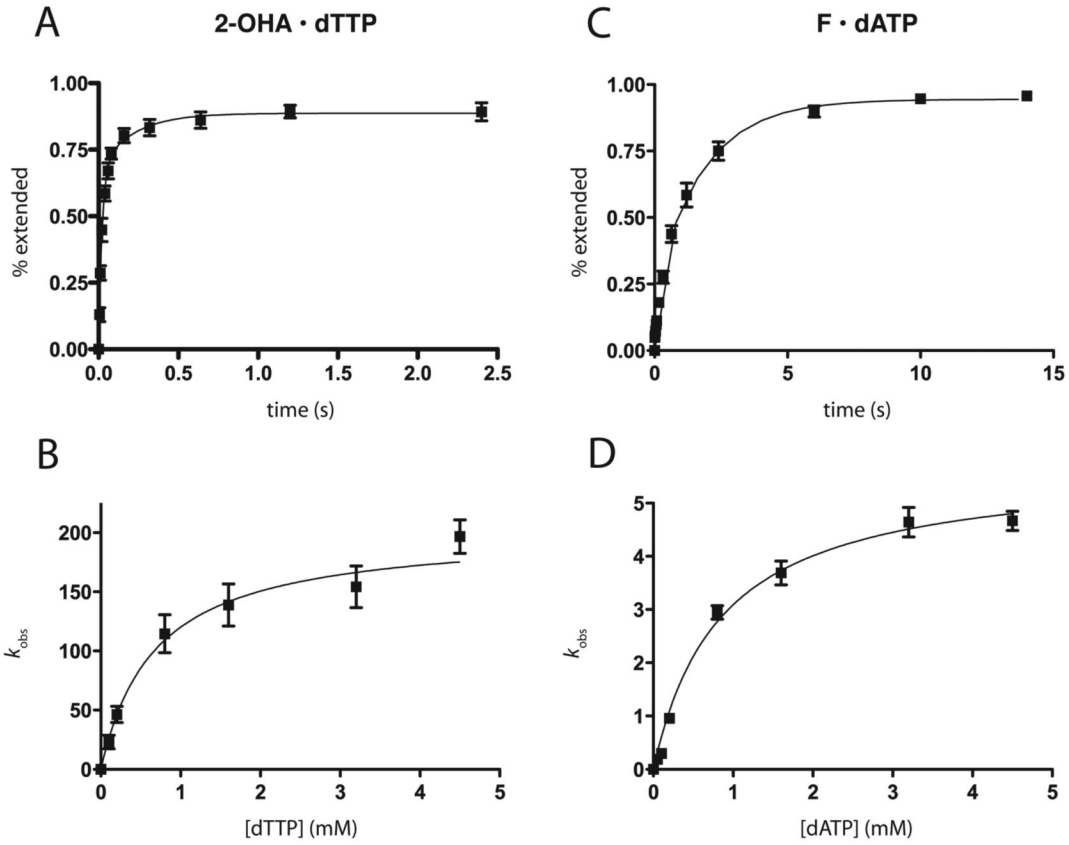

Figure 2.

Representative kinetic data. The product formation curve for incorporating 200 μM dTTP opposite 2-OHA by the L561A variant (A) was fit to a double exponential equation ($P=A(1-e^{-k_{fast}*t})+B(1-e^{-k_{slow}*t})$) and for incorporation of 200 μM dATP opposite F (C) was fit to a single exponential equation ($P=A(1-e^{-k*t})$). The rate constants for each reaction were plotted against dNTP concentrations and fit to a square hyperbola ($k_{obs} = (k_{pol}\,[dNTP])/(K_{D,APP}\,[dNTP])$) for 2-OHA•dTMP (B) and F•dAMP (D).

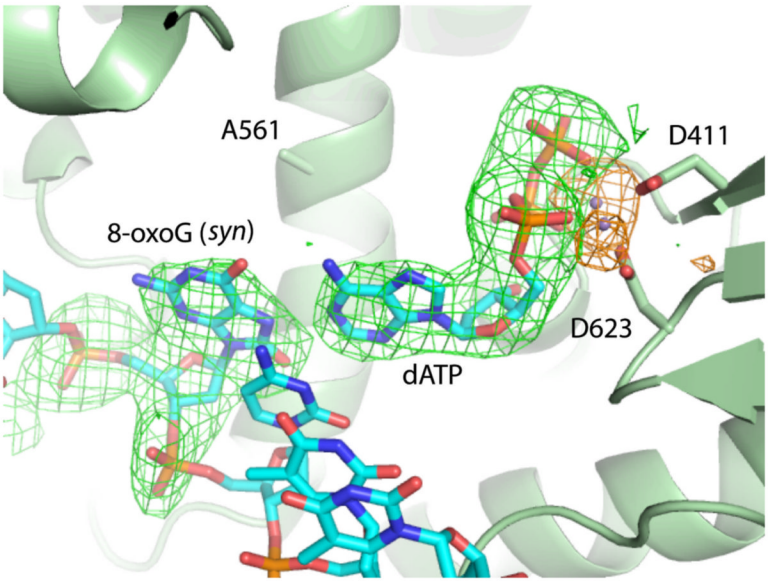

Figure 3.
The 8-oxoG•dATP mispair in the active site of the RB69 DNA polymerase. An Fo-Fc map is shown (green; contoured at 2.5 σ), along with an anomalous difference Fourier map (orange, contoured at 4.5 σ) pinpointing the location of the two manganese ions (purple spheres). dATP fits the density in a normal *anti* conformation while the electron density shows clear evidence that 8-oxoG adopts a *syn* conformation. The primer strand of DNA has been omitted to aid in clarity.

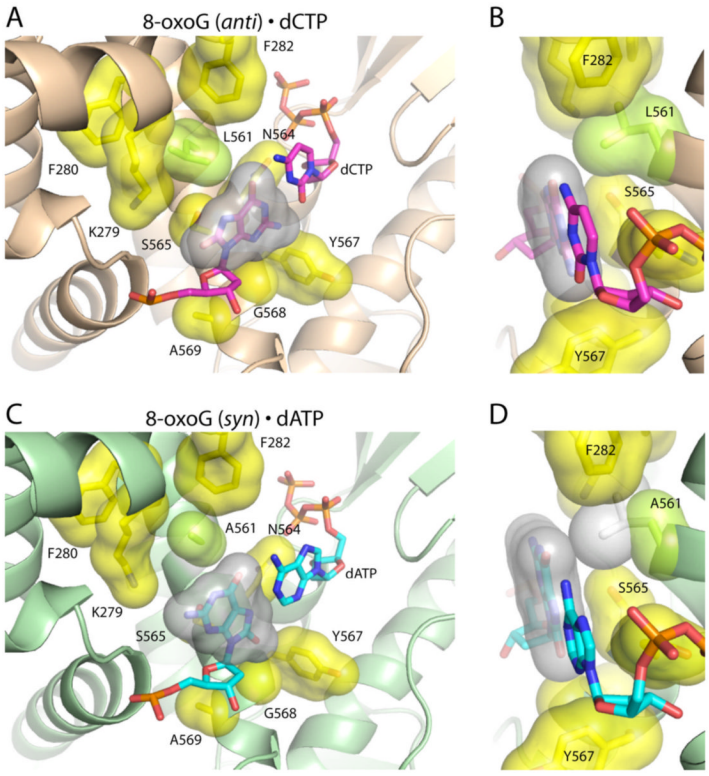

Figure 4.

Comparison of 8-oxoG•dNTP ternary complexes. In these images, the structures have been aligned using the α-carbons of the palm domain (residues 383-468 and 573-729). The duplex DNA from all structures was omitted for the sake of clarity. (A) The ternary complex with a 8-oxoG *(anti)*•dCTP base pair (PDB ID: 1Q9Y) (9) is shown as a cartoon (tan) and the nascent base pair is shown in magenta. Van der Waals surfaces are shown for the residues forming the nucleotide binding pocket (yellow), 8-oxoG (gray) and L561 (light green). (B) An orthogonal view to (A) illustrating the proximity between 8-oxoG (*anti*) and L561. (C) The ternary complex of 8-oxoG (*syn*)•dATP from this work is shown in pale green and the nascent base pair in cyan. (D) An orthogonal view to (C) predicting an unfavorable contact between 8-oxoG (*syn*) and A561. In this view a leucine residue (pale gray) has been modeled onto the alanine at position 561 to show the unfavorable interaction that may develop between 8-oxoG (*syn*) and L561.

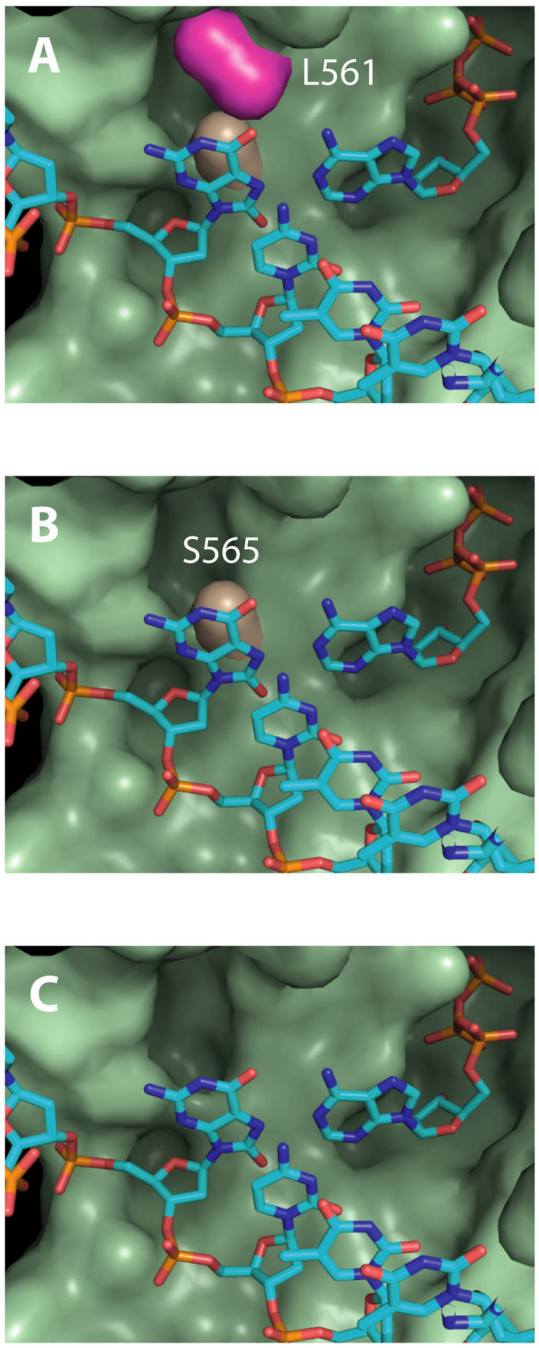

Figure 5.

A cavity is exposed when leucine 561 is substituted with alanine. (A) The polymerase domain of the current work is shown as a pale green surface, a modeled leucine 561 is shown in magenta and serine 565 is shown in tan. The leucine and serine residues block the cavity in this image. (B) Removal of the leucine residue opens up this cavity and may provide an opportunity for alternate template configurations to occur during DNA synthesis. (C) Mutation of serine 565 to glycine as described previously (52) shows an even more exposed cavity.

Table 1

Kinetic parameters for replication of undamaged and damaged DNA by the RB69 wild type (WT) and L561A DNA polymerases.

		k_{pol} (S^{-1})			K_D (mM)	
	L561A	**WT**[b]	**L561A/WT**	**L561A**	**WT**	**L561A/WT**
T●dAMP [a]	251.6 (8.5)	228.8 (10.07)	1.1 (0.06)	0.013 (0.002)	0.021 (0.004)	0.6 (0.15)
8-oxoG●dAMP	33.2 (2.4)	6.0 (0.27)	**6 (0.47)** [c]	0.86 (0.2)	1.14 (0.15)	0.8 (0.2)
8-oxoG●dCMP	75 (4.4)	135.8 (13.01)	0.6 (0.06)	0.2 (0.05)	0.65 (0.23)	0.3 (0.13)
8-oxoG●dGMP	0.29 (0.02)	0.0061 (0.0005)	**48 (5.1)**	1.46 (0.21)	1.11 (0.24)	1.3 (0.34)
8-oxoG●dTMP	0.26 (0.008)	0.026 (0.002)	**10 (0.83)**	3.14 (0.19)	1.91 (0.29)	1.6 (0.27)
2-OHA●dAMP	0.019 (0.001)	0.0008 (0.00007)	**24 (2.43)**	1.28 (0.24)	0.71 (0.24)	1.8 (0.7)
2-OHA●dCMP	0.066 (0.003)	0.0047 (0.0002)	**14 (0.86)**	1.16 (0.16)	0.89 (0.12)	1.3 (0.25)
2-OHA●dGMP	0.2 (0.02)	0.019 (0.002)	**11 (1.53)**	2.41 (0.48)	2.36 (0.52)	1.0 (0.3)
2-OHA●dTMP	201.7 (18.1)	101.3 (20.2)	2 (0.44)	0.68 (0.2)	1.67 (0.8)	0.4 (0.23)
F●dAMP	5.7 (0.3)	0.36 (0.02)	**16 (1.21)**	0.84 (0.13)	1.9 (0.24)	0.4 (0.23)
F●dCMP	0.1 (0.01)	0.0015 (0.0002)	**67 (11.11)**	4.21 (0.96)	3.46 (0.74)	1.2 (0.38)
F●dGMP	1.74 (0.13)	0.063 (0.005)	**28 (3.01)**	2.31 (0.4)	1.59 (0.32)	1.5 (0.39)
F●dTMP	0.48 (0.03)	0.0039 (0.0006)	**123 (20.43)**	2.65 (0.37)	2.36 (0.72)	1.1 (0.38)

[a] The first column is the templating base●incorporated nucleotide.

[b] wild type.

[c] The values in bold are those in which the difference between L561A and WT is greater than 5-fold.

Table 2

Insertion specificity for the most efficient translesion reactions catalyzed by the RB69 L561A and wild type (WT) DNA polymerases.

	k_{pol}/K_D (s^{-1} mM^{-1}) [a]		
	L561A	**WT**	**L561A/WT**
T●dAMP [b]	19353	10895	1.8
2-OHA●dTMP	297	61	4.9
F●dAMP	6.8	.2	35.8
F●dGMP	.75	.04	19.0
Efficiency dAMP/dGMP	9	5	
8-oxoG●dCMP	375	209	1.8
8-oxoG●dAMP	38.6	5.3	7.3
Efficiency dCMP/dAMP	10	39	

[a] The k_{pol} and $K_{D,APP}$ values are from Table 1.

[b] The templating base is given first and the incorporated nucleotide is given second.

Table 3

Data collection and refinement statistics

Data collection	
Space group	$P2_12_12_1$
Cell dimensions	
a, b, c (Å)	81.01, 121.0, 128.67
α, β, γ (°)	90, 90, 90
R_{merge}	.099 (.48)
$I / \sigma I$	17.5 (3.2)
Completeness (%)	98.4 (86.7)
Redundancy	7.0 (4.9)
Refinement	
Resolution (Å)	30 3.0
No. reflections	22682
R_{work} / R_{free} [a] (%)	24.8 / 29.7
No. atoms	
Protein	7369
DNA	680
Mn^{2+}	3
Water	12
B-factors (Å^2)	
Protein	97
DNA	74
Mn^{2+}	60
Water	45
R.m.s. deviations	
Bond lengths (Å)	0.007
Bond angles (°)	1.11

The values in parentheses are for the highest resolution bin.

[a] Rfree was calculated with 5% of the reflections not used in refinement